NeuroImage 124 (2016) 509–517

Contents lists available at ScienceDirect

NeuroImage

journal homepage: www.elsevier.com/locate/ynimg

Automated TMS hotspot-hunting using a closed loop threshold-based algorithm

Jonna Meincke, Manuel Hewitt, Giorgi Batsikadze, David Liebetanz *

Department of Clinical Neurophysiology, Georg August University of Göttingen, University Medical Center, 37075 Göttingen, Germany

ARTICLE INFO

Article history:
Received 5 June 2015
Accepted 7 September 2015
Available online 15 September 2015

Keywords:
Transcranial magnetic stimulation
TMS reliability
Accuracy
Neuronavigation
Robot
Automation
Threshold
Hotspot
Mapping

ABSTRACT

Background: Although neuronavigation is increasingly used for optimizing coil positioning, the inter-session reliability of hotspot location remains unsatisfactory, probably due to the variability of motor evoked potentials (MEPs) and residual investigator bias.
Purpose: To increase the reliability and accuracy of hotspot location we introduce a novel automated hotspot-hunting procedure (AHH).
Methods: AHH is based on resting motor thresholds (RMTs) instead of MEP amplitudes. By combining robotic coil positioning with a closed loop target search algorithm AHH runs independently from the investigator. AHH first identifies all targets with an RMT below a defined intensity of stimulator output (MEP-positive) and then locates the motor hotspot of a target muscle by measuring RMTs at all identified MEP-positive targets. Results were compared to robotic MEP amplitude TMS mapping (MAM) using a 7×7 predefined target grid and suprathreshold intensities and manual hotspot search (MHS). Sequence of stimulation was randomized from pulse to pulse in AHH and MAM. Each procedure was tested in 8 subjects.
Results: Inter-session CoG shift was significantly reduced with AHH (1.4 mm (SEM: 0.4)) as compared to MAM (7.0 mm (SEM: 1.8)) ($p = 0.018$) and MHS (9.6 mm (SEM: 2.2)) ($p = 0.007$). No statistical difference was observed between MAM and MHS. RMTs were reliable between sessions.
Conclusion: Our method represents the first fully automated, i.e. investigator-independent, TMS hotspot-hunting procedure. Measuring RMTs instead of MEP amplitudes leads to significantly increased accuracy and reliability of CoG locations. Moreover, by assessing thresholds AHH is the first procedure to fulfill the original hotspot definition.

Introduction

Transcranial magnetic stimulation (TMS) (Barker et al., 1985) is a frequently used tool for the non-invasive investigation of the human motor cortex. Besides its use for the identification of cortical representation areas of muscles, TMS is commonly applied in studies that aim at identifying factors that modulate or influence cortical excitability (Grundey et al., 2012; Lang et al., 2013). For both purposes, the accurate and reliable location of the optimal position for TMS (i.e. motor hotspot) is a substantial part.

However, although studies have recently aimed at improving the reliability of TMS mapping, the inter-session shift of hotspot location is still unsatisfactory ranging from several millimeters (Ngomo et al., 2012) to centimeters (Cincotta et al., 2010; Gugino et al., 2001; Julkunen et al., 2009; Malcolm et al., 2006; Weiss et al., 2013). Since inaccurate coil positioning (Brasil-Neto et al., 1992; Ellaway et al., 1998; Mills et al., 1992; Schmidt et al., 2015), varying distances between the TMS coil and scalp (Richter et al., 2013a), coil rotation and stimulation intensity (Bashir et al., 2013; Di Lazzaro et al., 1998a; Di Lazzaro et al., 2001; Richter et al., 2013a) strongly affect TMS measurements, different neuronavigated systems have been introduced to increase accuracy of positioning (Julkunen et al., 2009; Weiss et al., 2013). However, in addition to the mentioned physical factors, physiological factors, such as voluntary muscle activation (Di Lazzaro et al., 1998b), individual neuroanatomy, differences within the conductivity of brain tissues (Thielscher et al., 2011), time-dependent fluctuations in the subjects' cortical excitability (Lang et al., 2011) and the high variability of motor evoked potentials (MEPs) (Jung et al., 2010; Kiers et al., 1993; Wassermann, 2002).

To overcome the drawbacks of manual TMS mapping and to improve the reliability, we introduce a novel investigator-independent and automated TMS motor hotspot-hunting procedure (AHH). Robotic TMS increases accuracy in positioning (Kantelhardt et al., 2010; Lancaster et al., 2004) and enables automated experiments. Therefore, the influence of the investigator is minimized. To avoid that time-dependent fluctuations in the subjects' cortical excitability bias the results, the stimulation sequence was randomized during the entire experiment. To further reduce the influence of the variability of MEP

* Corresponding author at: Universitätsmedizin Göttingen, Robert-Koch-Straße 40, 37075 Göttingen, Germany.
E-mail address: dliebet@gwdg.de (D. Liebetanz).

http://dx.doi.org/10.1016/j.neuroimage.2015.09.013
1053-8119/

amplitudes on hotspot location we used resting motor thresholds (RMTs) instead of MEP amplitudes as the output parameter. In contrast to MEP amplitudes RMTs remain more stable over time (Lang et al., 2011; Malcolm et al., 2006). Furthermore, AHH is the first TMS procedure introduced to date that fulfills the original hotspot definition, defining the hotspot as the position on the scalp where the threshold is lowest and latency shortest (Rossini et al., 1994). As a feasible procedure for hotspot location has not been available so far (Siebner and Ziemann, 2014) the motor hotspot is usually defined as the position on the scalp where the largest and most consistent MEP amplitudes are evoked with a given stimulation intensity (van de Ruit et al., 2014; Volz et al., 2014).

Materials and methods

Subjects

The study was approved by the ethics committee of the University of Göttingen and complies with the Declaration of Helsinki. Informed written consent was obtained from 11 healthy subjects (3 males) aged 25–40 years (mean: 29 years). All of them were right-handed according to the Edinburgh handedness inventory (Oldfield, 1971).

Experimental setup

For TMS we used a Magstim 200^2 magnetic pulse stimulator and a 70 mm figure-of-eight coil with a peak magnetic field of 2.2 T at the maximum stimulator output intensity (MSO) (Magstim Company, Whitland, UK). For electromyography (EMG) recordings we used surface electrodes (Ag–AgCl) in a belly-tendon montage. The signal was amplified and band-pass filtered from 2 to 2000 Hz (Digitimer D360, Digitimer Ltd.). An A/D converter (CED micro1401 mkII, Cambridge Electronic Design) sampled the signal at 5000 Hz. Software (Signal v4, CED) recorded MEPs on a standard PC.

Prior to the TMS experiments, each subject participated in a magnetic resonance imaging (MRI) scanning session (T1-weighted 3D turbo-fast low-angle shot (FLASH) anatomical image at 1 mm^3 isotropic resolution) to acquire cranial MRI data (3-T Magnetom Trio, Siemens, Erlangen, Germany).

From the MRI data a model of the head surface was created in the robot navigation software (Smartmove, ANT, Enschede, Netherlands). For TMS, a robot (Adept Viper s850, Adept Technology Inc., Livermore, CA, USA) positioned the coil tangentially over the scalp with a rotation angle of 45° in the sagittal plane. With respect to the six degrees of freedom of movement, the positional error of the robot is ± 0.02 mm. To prevent that inhibitory or facilitatory effects from previous pulses influence the recordings (Kiers et al., 1993) we set the minimum inter-stimulus interval to 5 s. However, the actual inter-stimulus interval varied between 5 and 8 s depending on distance between the stimulated targets due to the movement speed of the robot. Smartmove controlled the movement of the robot for exact coil positioning. Additionally, it is used to register the subjects' head to a reflective marker of an optical tracking system (positional error: ± 0.5 mm) (Polaris Vicra, NDI Medical, Waterloo, Ontario, Canada) to allow for compensation of head movements. The same software was used for target creation and positioning.

Goal of the study

The goal of the study was to accurately and reliably identify the position on the scalp where the threshold for a target muscle is lowest, i.e. the motor hotspot (Rossini et al., 1994). For this purpose we developed a novel automated and investigator-independent hotspot-hunting procedure (AHH). We further compared AHH to a standard manual hotspot search (MHS) and a robotized standard MEP amplitude based TMS mapping experiment (MAM).

Experimental design

AHH, MAM and MHS were conducted in 8 subjects. 5 subjects participated in all three experiments (2 male), 3 subjects only in the AHH experiment (1 male) and the other 3 only in the MAM and MHS experiments (2 males). The first dorsal interosseus muscle (FDI) was used as the target muscle for all experiments. Experiments were performed with the muscle at rest.

For each procedure two consecutive sessions (one after the other on the same day) were performed. The experimental setup remained unchanged between sessions to exclude interfering factors. The neuronavigation marker and the electrodes remained on the subject and subjects were not allowed to touch or move the neuronavigation marker. Experiments paused every 15 min and there was a break between the sessions. The subjects determined the duration of the breaks and were allowed to move during the breaks. To keep the subjects alert, subjects were allowed to watch documentaries during the experiments.

Automated hotspot-hunting procedure (AHH)

A self-written software script (in Signal v4) controlled the experiment. After the starting parameters were set, AHH ran automatically so that further interaction by the investigator was not necessary. Starting parameters were a predefined grid of potential targets, a starting target in the center of the grid and a given initial maximum stimulation intensity (MSI). The grid of potential targets covered most of the left hemisphere (grid with 7 mm spacing; 17 × 17). It was placed between the vertex and the auricle and was centered in the middle of the medioauricular line. Theoretically, the maximum stimulation intensity is the maximum stimulator output. However, to not extend the time of the experiment and to reduce discomfort we used a lower maximum stimulation intensity. Due to the observation that males generally have higher thresholds than females MSI was set to 50% MSO for males and 45% MSO for females. Thresholds were determined with the maximum likelihood threshold-hunting algorithm (Awiszus, 2003). This probability-based method for the calculation of the estimated threshold consists of delivering TMS pulses with different intensities. Depending on the resulting MEPs (< or ≥ 50 μV) the algorithm calculates an estimated threshold. The stimulation intensity for the subsequent stimulus is then automatically set to this threshold. This process can be repeated an infinite number of times. The more pulses are applied, the higher the probability that the estimated threshold corresponds to the real threshold. At least 14 stimuli are required for accurate threshold determination(Awiszus, 2011). As a compromise between the time needed and data quality/error AHH ended after a total of 15 stimuli were applied at each target (see below). To further assure a more robust RMT determination within 15 pulses and over the relatively long period of time of the experiment, we added an online outlier control into the algorithm, which automatically controlled if the estimated thresholds converged at each target. If the estimated thresholds at a target were increasing or decreasing monotonically for the last 5 pulses, the preceding MEP (at the respective target) was classified as an outlier. In this case the software automatically discarded the last 6 data points (rollback) (Fig. 1).

Instead of assessing the RMT at one target and then advancing to the next target, the sequence of stimulation was randomized for every pulse during the entire experiment. After each TMS pulse, the robot moved the coil to the next randomly chosen target.

Overall, the entire AHH consisted of three phases (Figs. 2 and 3) with each phase covering a part of the maximum likelihood threshold-hunting measurement. In all phases, targets were picked from a target pool, which was populated or emptied by rules depending on the phase. In the first two phases of the experiment, targets were tested if their threshold was below or above MSI A target was defined as being MEP-positive if TMS at or below MSI evoked an MEP amplitude of ≥ 50 μV. Targets where two successive stimuli with MSI did not evoke

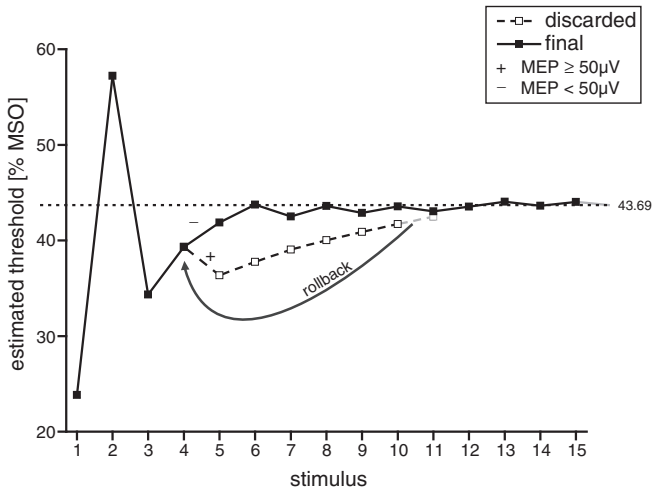

Fig. 1. Threshold-hunting and online outlier control. Course of the estimated threshold (line) at a single target of session 2 in subject 3. As there was no convergence of the estimated threshold after the last 5 stimuli at the stimulus 10, the previous MEP (at stimulus 5) was defined as an outlier. The outlier and the subsequent stimuli were discarded (rollback).

an MEP ≥ 50 μV were classified as being MEP-negative and excluded from further measurements.

The objective of phase 1 was to localize a first MEP-positive target. The initial target pool only consisted of the starting target. This target was tested if it was MEP-positive or MEP-negative. If it was MEP-positive, phase 1 ended immediately. If it was MEP-negative, the target pool was populated with its adjacent targets (anterior, posterior, lateral and medial) from the predefined target grid. Pulses were applied to the targets of the target pool in a random order until it could be determined if they were MEP-positive or MEP-negative. If one or more target(s) was/were MEP-positive, phase 1 ended. If they were all MEP-negative, the target pool was populated again with the respective adjacent targets and testing was resumed until at least one MEP-positive target was identified.

Phase 2 aimed to identify all of the MEP-positive targets adjacent to the MEP-positive target(s) from phase 1. At the beginning of phase 2, the target pool included the unmeasured targets adjacent to the MEP-positive target(s) from phase 1. For each TMS pulse, a target was randomly picked from the target pool. If a target could be identified as being MEP-positive, it was removed from the target pool of phase 2 and its adjacent unmeasured targets were added to the target pool. If a target was MEP-negative, it was removed from the target pool without adding new targets. This procedure was repeated until the target pool was empty. At the end of phase 2, all targets with a threshold below MSI (MEP-positive) have been identified.

In phase 3, threshold determination was finalized at all MEP-positive targets identified in phase 1 and 2. To assure that the experiment included a similar number of targets in all subjects and to not unnecessarily lengthen the time of the experiment we adjusted the MSI before starting phase 3 by introducing a cut-off with the following formula:

$$MSI_{new} \approx MSI - \left(\Sigma_{MEP-positive\ \ targets}/10\right); \text{for all } \Sigma_{MEP-positive\ targets} \geq 30.$$

In subjects with low thresholds, the predefined maximum stimulation intensity resulted in a higher number of MEP-positive targets as compared to subjects with lower thresholds. Therefore, the adjustment was generally necessary in subjects with low thresholds. In these subjects, targets at the edge of the hotspot area (distant from the motor hotspot) were more likely identified as being MEP-positive and a higher number of targets were identified as MEP-positive. The more MEP-positive targets were identified, the more the maximum stimulation intensity was reduced.

For example, if the number of MEP-positive targets was 24, the MSI remained unchanged, but if 37 targets were identified as MEP-positive, it was reduced by 4 %. If the number of MEP-positive targets was less than 20, phase 1 and 2 would have been repeated with a higher MSI. After adjusting the stimulation intensity, the respective targets were—just like in subjects with higher thresholds—classified as being MEP-negative. As this procedure did not affect measurements at the remaining targets (hotspot area), the hotspot location was not influenced.

The sequence of TMS stimuli was also randomized in phase 3. Phase 3 ended after a total of 15 stimuli were delivered per MEP-positive target.

In session 2, the adjusted maximum stimulation intensity from session 1 was used from the beginning of phase 1 to not unnecessarily extend the time of phase 2 in session 2.

Manual hotspot search (MHS) and robotized MEP amplitude mapping procedures (MAM)

A highly experienced investigator in the field of TMS performed the MHS experiment. He was instructed to locate the optimal position for TMS (i.e. the motor hotspot) and to determine the RMT as precisely as possible. The experiment was blinded, i.e. the investigator did not know the stimulation intensities. He instructed a second investigator to decrease or increase the stimulation intensity. At the beginning, the stimulation intensity was set to a random value between 30 and 40% MSO. The inter-stimulus interval was 5 s.

For the MHS the investigator applied TMS pulses at different scalp positions where he expected the FDI hotspot to be located. If after ~10–20 pulses no MEP was observed, the stimulation intensity was increased by 5% MSO and the procedure was repeated. Once the optimal position was identified the stimulation intensity was decreased until 50% of ~10–15 pulses showed an MEP of ≥50 μV. To assure that the position was correct, the investigator positioned the TMS coil at the adjacent scalp positions in order to look for a position with a lower threshold. The investigator marked the optimal position on the scalp with a non-permanent marker. Then this position was recorded in the neuronavigation software and the marking was removed.

The MHS was followed by the MAM. For this we used a predefined target grid (7 × 7, 7 mm spacing), which was centered on the manual hotspot of the previous experiment. The stimulation intensity was set to 120% of the previously determined RMT. Similar to AHH, the coil was positioned by a robot, the sequence of stimulation was randomized and the inter-stimulus interval was set to 5 s. To assure comparability between procedures we used the same setting and TMS system as used for AHH for the MAM control experiment. Also the total number of pulses per session was similar in the MAM control experiment (resulting in 10 pulses per target).

Data analysis

We used the estimated thresholds (RMT_i) (in case of AHH) and mean MEP amplitudes (in case of MAM) to calculate topographic maps of the hotspot areas. Data analysis was performed with Matlab (MathWorks, Natick, MA). The center of gravity (CoG) of the AHH was calculated using the following formula (Wassermann et al., 1992):

$$CoG = \Sigma v_{i*} x_i / \Sigma v_{i*}, \Sigma v_{i*} y_i / \Sigma v_{i*}; \text{with } v_i = MSI - RMT_i.$$

Centers of gravity of MAM results were calculated using the following formula:

$$CoG = \Sigma v_{i*} x_i / \Sigma v_{i*}, \Sigma v_{i*} y_i / \Sigma v_{i*}; \text{for all } v_i = MEP_{mean}.$$

The inter-session shifts in CoG location were calculated from the CoG coordinates. We used individual MRI coordinates without transforming the MRIs into a common space. Distances were measured in millimeter.

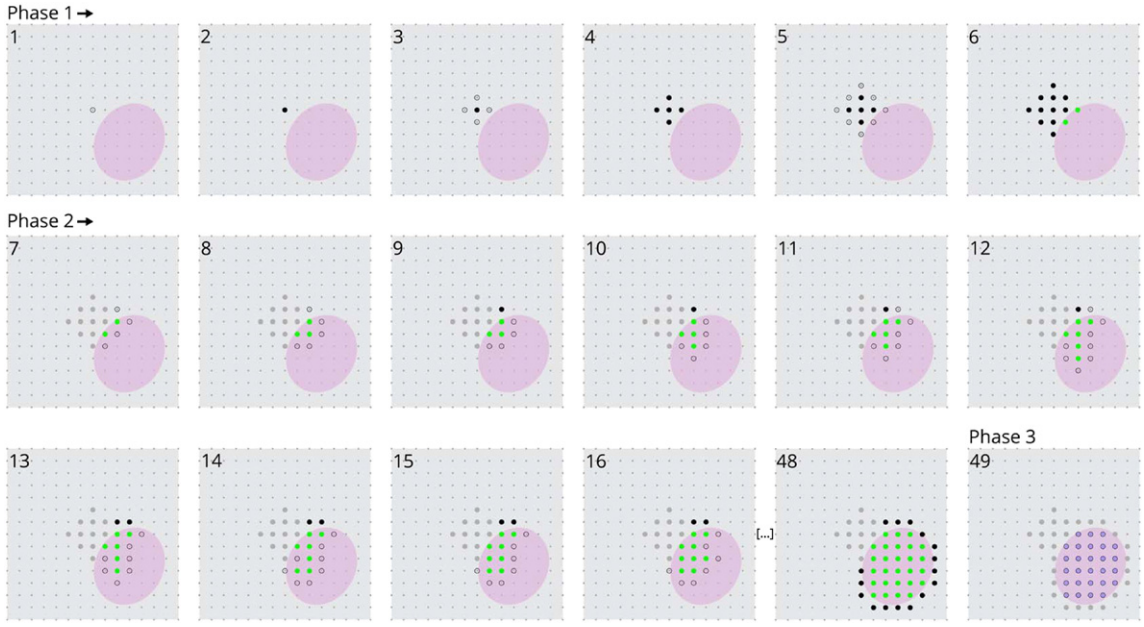

Fig. 2. Diagram of the hotspot-hunting algorithm. At the beginning of the experiment the location of the hotspot area (pink) is unknown. The experiment consists of 3 consecutive phases. In each of the three phases, the targets to be tested are randomly picked from a target pool (grey circles), which is populated or emptied by phase-dependent rules. Pulses were applied to the targets of the target pool in a random order until it could be determined if they were MEP-positive (green dots) or MEP-negative (black dots). At the beginning of phase 1 the target pool only consists of a starting target in the center of the grid (1). If it is MEP-negative (2), its adjacent targets are added to the pool (3) and testing is resumed until the pool is emptied (4). This procedure is repeated (5) until the first MEP-positive target(s) is/are identified (6). At the beginning of phase 2 the target pool consists of the (unmeasured) adjacent targets of the MEP positive target(s) from phase 1 (7). Targets that have already been tested (grey dots) are not tested again. In case a target is MEP-positive its adjacent targets are added to the pool (e.g. 8). This procedure is repeated until the target pool is emptied (48). In phase 3, RMT measurements continue at all targets from the pool. The target pool of phase 3 consists of the MEP-positive targets from phase 1 and 2 (blue circles) (49).

Statistical analysis was carried out in R (R foundation for statistical computing, version 3.1.2). We used the Shapiro–Wilks test to test for normal distribution. A one-way, single-measure, intra-class correlation coefficient (ICC) was used to test re-test reliability. ICC values > 0.75 were considered as reliable. We used a Student's t-test to explore differences between procedures of inter-session CoG shift and accuracy.

Results

Automated hotspot-hunting procedure (AHH)

An average AHH session took 66 min (SEM: 4) including breaks (Fig. 4). The average time for session 1 was 68 min (SEM: 4) and 65 min (SEM: 3) for session 2.

Phase 1 took 42 s (SEM: 3) on average. In 9 out of 12 sessions the starting target was the first MEP-positive target. In three sessions the target pool was expanded once and in one session it was expanded twice (Figs. 3 and 4) until the first MEP-positive target was identified. Phase 2, took on average 21 min (SEM: 2) in session 1 and 15 min (SEM: 1) in session 2. A mean of 52.8 (SEM: 4.6) targets were tested in session 1 and 48.3 (SEM: 2.1) in session 2. At the end of phase 2 an average of 31 (SEM: 3.5) targets in session 1 and 26.5 (SEM: 1.8) targets in session 2 were classified as MEP-positive. In phase 3 of session 1 the maximum stimulation intensity was reduced by means of the cut-off in 3 subjects. An average of 21.4 targets (SEM: 1.4) were MEP-positive at the end of phase 3. Phase 3 of the experiment took 47 min (SEM: 3) on average. An average of 8 rollbacks (SEM: 2) were performed per session (Figs. 1 and 4).

With AHH (Fig. 2) the FDI motor hotspot was located in all subjects (Figs. 3 and 5). The FDI cortical representation areas were mainly oval and with the longer axis extending from antero-medial to postero-lateral (Fig. 5). The difference in number of MEP-positive targets between sessions was 4.5 (SEM: 1.3) with significantly less MEP-positive targets in session 2.

The average shift of the CoGs between sessions calculated from the estimated RMTs after 15 pulses per target was 1.4 mm (SEM: 0.4). The average shift was 0.7 mm (SEM: 0.2) on the x-axis, 1.1 mm (SEM: 0.3) on the y-axis and 0.5 mm (SEM: 0.1) on the z-axis (Fig. 5). There was no session-dependent direction with respect to the CoG shift. The accuracy of the CoG locations depends on the number of pulses per target (Fig. 6). The accuracy reaches a maximum after about 9 pulses. The mean distance between the CoG locations after 9–14 pulses per target and the final CoG after 15 pulses was 0.4 mm (SEM: 0.02) (Fig. 6).

Minimum thresholds assessed by AHH were highly reliable between sessions (ICC = 0.97) with 36.8% MSO (SEM: 1.7) in session 1 and 36.1% MSO (SEM: 1.8) in session 2 (Fig. 3). The threshold varied by 1.1 % MSO (SEM: 0.2) between sessions. However, there was no systematic shift across subjects. The inter-session distance of the targets where the threshold was lowest (hotspot on grid) was on average 6.6 mm (SEM: 2.6) in 3-dimensional space.

Manual hotspot search (MHS)

The MHS took on average 9 min (SEM: 1) in session 1 and 9 min (SEM: 1) in session 2. The manual RMT determination was reliable between sessions (ICC = 0.98). RMT was on average 34.3% MSO (SEM: 2.4) in session 1 and 34.8% MSO (SEM: 2.4) in session 2. Mean RMT difference between sessions was 1% MSO (SEM: 0.3). There was no systematic shift across subjects. Average inter-session distance of the manually determined hotspots was 9.6 mm (SEM: 2.2). The Welch two-sample t-test revealed a significantly higher CoG shift with MHS as compared to AHH ($p = 0.007$).

MEP amplitude TMS mapping (MAM)

The MAM took on average 62 min (SEM: 2) with a mean of 538 (SEM: 11) pulses per session. With MAM the inter-session CoG shift was on average 7.0 mm (SEM: 1.8). The average shift per axis was 4.4 mm (SEM: 1.0) for the x-axis, 3.9 mm (SEM: 1.9) for the y-axis

and 1.6 mm (SEM: 0.5) for the z-axis. The Welch two-sample t-test showed that the inter-session CoG shift was significantly higher with MAM as compared to AHH ($p = 0.018$). No statistical difference was observed between MAM and MHS. The accuracy of CoG locations depended on the number of pulses per target.

The average number of targets with a mean MEP amplitude of ≥ 25 μV (noise level) was 25.5 (SEM: 2.0) in session 1 and 23.9 (SEM: 1.9) in session 2. The mean inter-session difference of the number of targets with an MEP was 3.4 (SEM: 1.1). However, there was no systematic difference. Sizes of the hotspot areas were not reliable between sessions (ICC = 0.67).

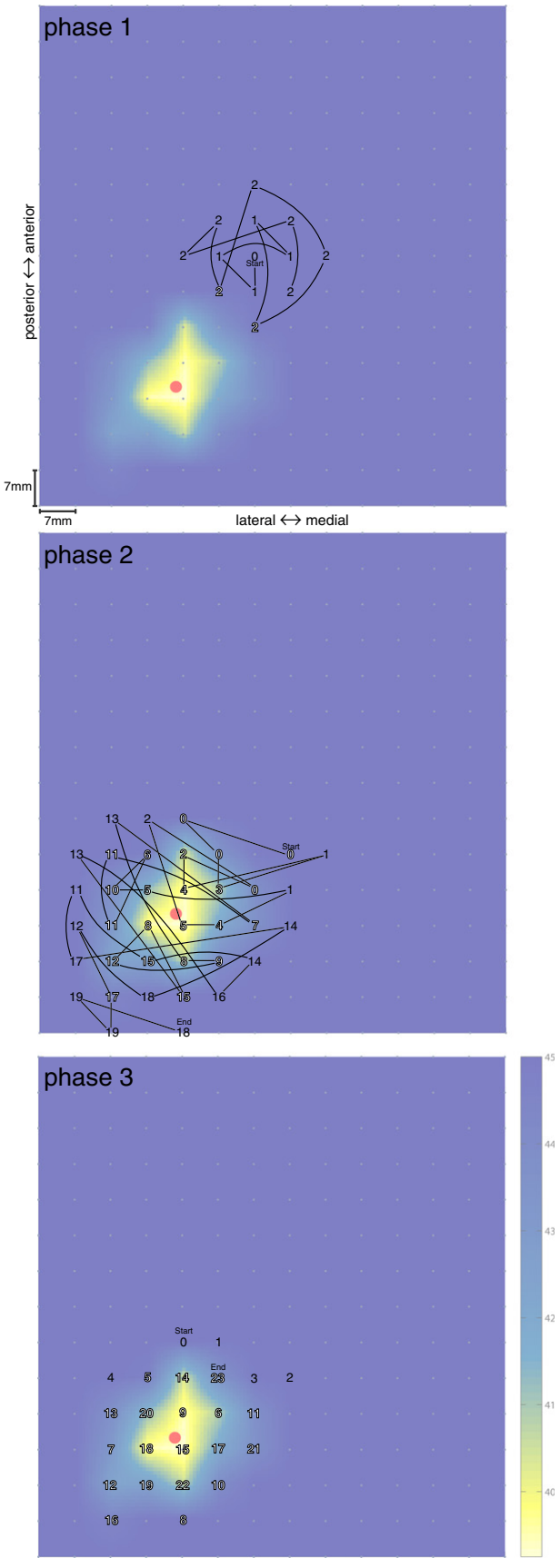

Discussion

In the presented proof of concept study we introduce a novel automated TMS hotspot hunting procedure (AHH). The inter-session CoG shift was significantly reduced with AHH as compared to MAM ($p = 0.018$) and MHS ($p = 0.007$). Since AHH and MAM both used robotic coil positioning, the similar setup, a similar coil rotation angle and a randomized stimulation sequence, our results point to a high impact of the output parameter on accuracy and reliability of TMS hotspot location.

Accuracy, inter-session reliability and advantages of AHH

With AHH and using the described stimulation parameters and experimental setting the FDI motor hotspot was precisely located in all subjects. High accuracy and inter-session reliability of CoG location and minimum RMTs were achieved. This underlines the high precision of the introduced AHH. Within 3-dimensional space the accuracy of CoG locations was in the range of 0.5 mm. The inter-session shift of the CoGs was 1.4 mm.

In contrast, in general an average CoG shift in the range of centimeters is reported for conventional (manual) mapping procedures (Weiss et al., 2013; Wolf et al., 2004). The observed advantage of AHH is probably related to several factors.

We used an automated robot-aided system for coil positioning, which assures high accuracy with respect to the six degrees of freedom of the TMS coil (Kantelhardt et al., 2010). Compared to manual coil positioning, AHH therefore excludes influences of inaccurate coil positioning, which have already been identified as affecting TMS measurements (Conforto et al., 2004; Julkunen et al., 2009; Richter et al., 2013a; Volz et al., 2014). Besides controlling for the exact stimulation site and rotation angle, the robot's tracking mode also maintains a constant distance between scalp and TMS coil. This reduces deviations of the electric field induced by TMS (Richter et al., 2013b). The robotic system for coil positioning further enables that the stimulation sequence is entirely randomized, which is impractical in case of manual coil positioning, where pulses are usually applied consecutively at a given grid point (Littmann et al., 2013; Malcolm et al., 2006) or in a predefined order (Lotze et al., 2003). Randomization has the advantage to distribute fluctuations in the subjects' excitability over all targets and over the course of the entire experiment.

However, the most important difference to all previously reported TMS hotspot location procedures is the use of RMTs instead of MEP amplitudes as the output parameter. Therefore, AHH allows hotspot identification complying with the original hotspot definition (Rossini et al., 1994). RMT values remain also more stable over time (Lang et al., 2011; Malcolm et al., 2006; Wolf et al., 2004) compared to the high

Fig. 3. Process and result of hotspot-hunting in a single subject.Process of hotspot-hunting projected onto a heat map and CoG location (red dot) of subject 3 (session 2). Phase 1 started at the starting target (0). The first MEP-positive targets (white numbers) were located after expanding the target pool twice (first 1 then 2). Stimuli were applied in a random order with lines indicating the order of targets which where identified as MEP-positive or MEP-negative. At the beginning of phase 2, the target pool consisted of the adjacent targets of the MEP-positive target(s) from phase 1 (0). 37 targets were tested until 22 MEP-positive were identified. Numbers indicate the expansion order of the target pool. In phase 3 threshold-hunting was finalized at all MEP-positive targets. 5 previously MEP-positive targets were identified as MEP-negative (black numbers) in phase 3 and removed from the pool.

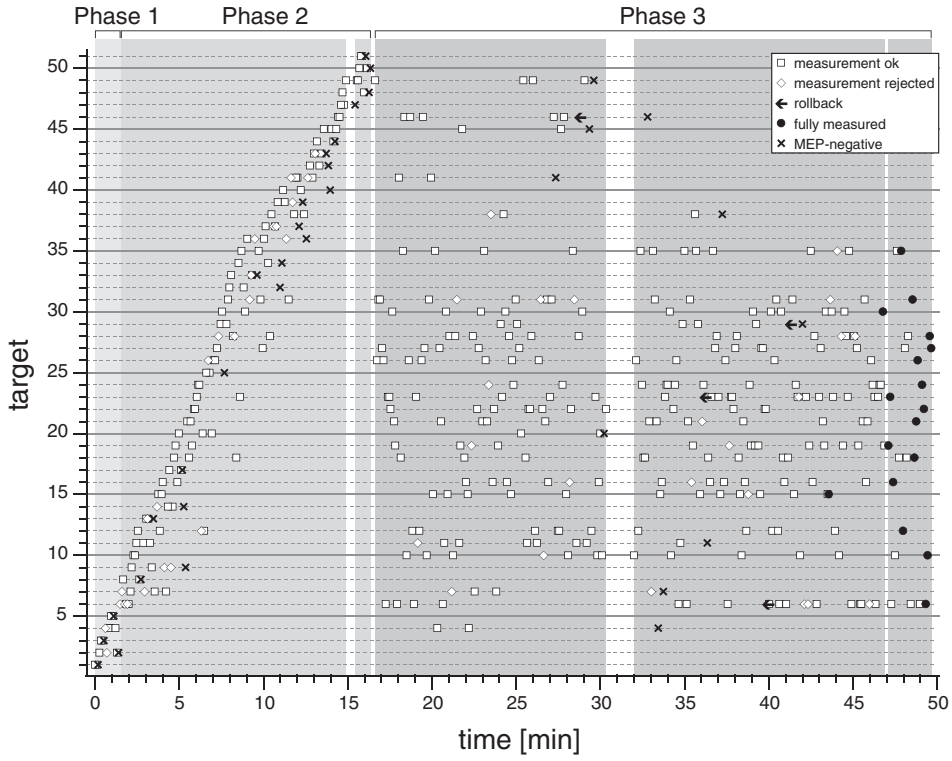

Fig. 4. Experiment timeline. Timeline of the stimuli of an experiment (subject 3, session 1) showing the different phases of the hotspot-hunting procedure (breaks are shown in white). In phase 1 and 2 an increasing number of targets have been tested by the algorithm within 16 min. MEP-negative targets are not further investigated. The stimulation at MEP-positive targets resumes in phase 3. In phase 3 stimuli are applied to all MEP-positive targets found in phase 1 and 2 until they are either reclassified as MEP-negative or until they are fully measured with 15 stimuli. The final stimulus per target is applied in the last 7 min of the experiment. Some measurements are rejected due to preinnervation of the muscle. After rollbacks previous stimuli are discarded and the measurement is repeated.

natural variability of MEP (Wassermann, 2002). A strong dependency of the accuracy and reliability of the CoG location on the output parameter is supported by the results of our MAM control experiment. To enable a direct comparison between the output parameters we used a similar setting and experimental design (similar number of stimuli, robotic coil positioning, similar inter-stimulus interval, similar spacing between targets) for the MAM control experiment. Here, the accuracy was significantly lower and inter-session CoG shift significantly higher regardless of also using a robotized coil positioning and a randomized stimulation sequence.

Measuring RMTs instead of MEPs has the additional advantage that the stimulation intensities applied at the majority of targets are considerably lower (near threshold intensity) as for MEP amplitude TMS mapping. Discomfort during the experiments is therefore reduced. Although our results revealed a clear advantage of AHH over MAM in terms of accuracy and reliability of CoG location a direct comparison of the results of both procedures is limited as AHH and MAM likely activate different cell populations by means of the different stimulation intensities used (Di Lazzaro et al., 1998a; Di Lazzaro and Ziemann, 2013).

Another innovation of AHH is the closed loop target search algorithm. In combination with robotic coil positioning, it enables automated and investigator-independent experiments, excluding any investigator bias. No prior information, such as approximate hotspot location, is required. The target search algorithm automatically searches for all targets with a threshold below the maximum stimulation intensity instead of measuring a predefined target grid. This has the additional benefit that MEP-negative targets are automatically excluded from the target pool during the experiment. The maximum number of pulses is therefore only applied at targets within the hotspot area, i.e. at MEP-positive targets. In contrast, conventional procedures generally require a target grid with a predefined size that is large enough to cover the entire hotspot area (usually between 5 × 5 cm and 7 × 7 cm) (Guerra et al., 2014; Malcolm et al., 2006). To position the grid and to set the stimulation intensity most conventional TMS mapping procedures require a manual hotspot search and RMT determination (Malcolm et al., 2006; Sparing et al., 2008; Wassermann et al., 1994). Moreover, in contrast to AHH conventional TMS mapping has the disadvantage that all targets from the grid are fully measured regardless of whether MEPs are elicited or not.

Perspectives

The results of this proof of concept study demonstrate that AHH leads to more accurate and reliable CoG location as compared to MAM. A high grade of accuracy was achieved in all subjects. Our results show that the accuracy of CoG location increases depending on the number of pulses per target. Interestingly, a floor effect was already achieved after 9 pulses per MEP-positive target (Fig. 6). A further addition of stimuli per target did, not further improve the accuracy of the CoG location. The remaining inaccuracy is most probably a result of three factors. Firstly, the magnetic stimulator has the drawback that the stimulation intensities can be only changed in steps of 1% of the MSO, resulting in a comparatively rough RMT determination. Secondly, the spacing between targets used here was higher than the precision of the system. Higher accuracy of CoG locations could therefore be achieved by introducing decimal degrees of stimulator output and/or a shorter distance between targets. Thirdly, despite the efforts we made to keep the subjects alert, the level of attention of the subjects could have slightly changed during the experiments and therefore influenced the comparison between sessions. However, a strong influence of this on the AHH results is unlikely as RMTs remain stable over the day and, in contrast to other TMS parameters, RMTs are only insignificantly affected by additional factors (Doeltgen and Ridding, 2010; Lang et al., 2011; Tamm et al., 2009). Moreover, the stimulation sequence was

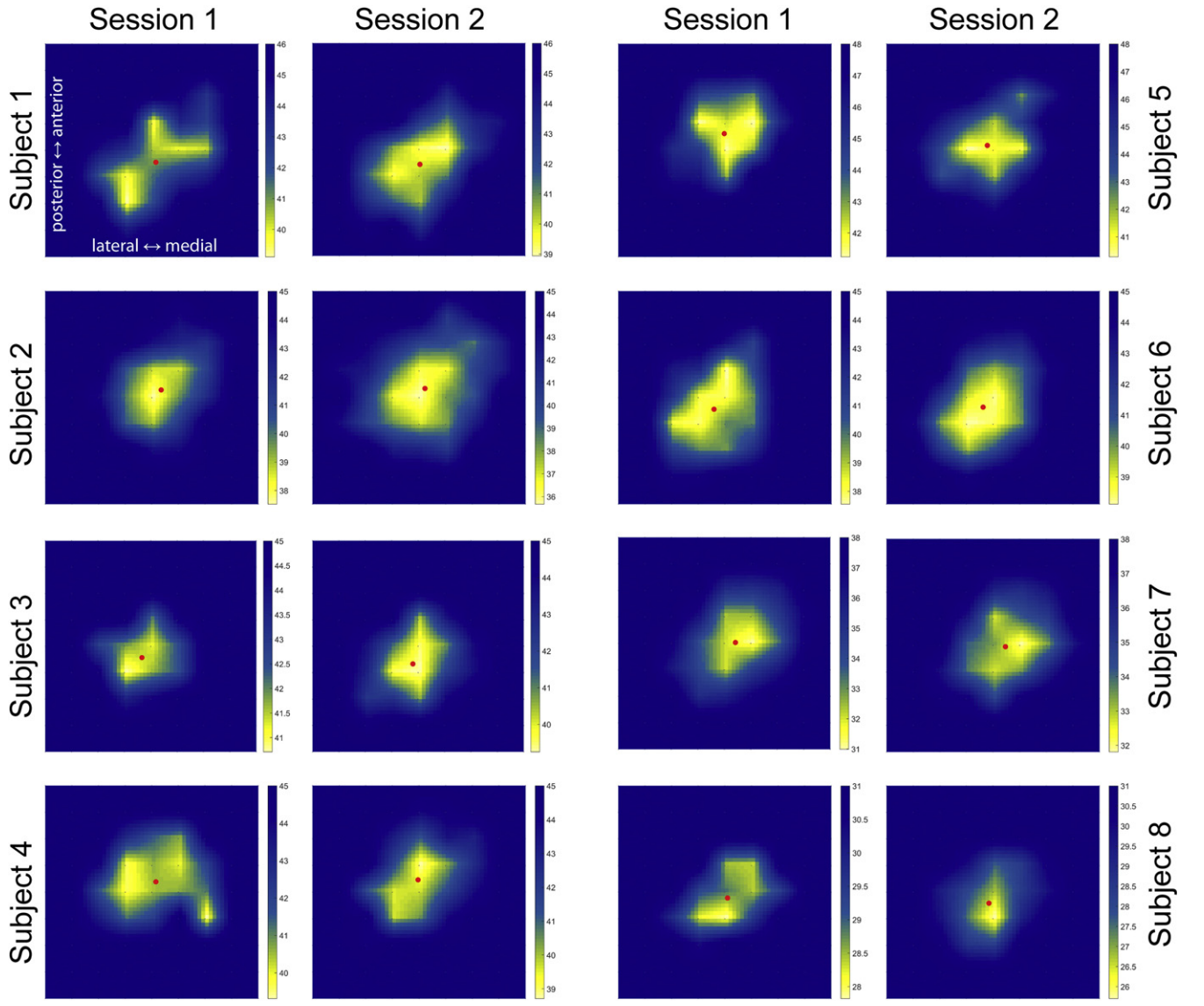

Fig. 5. Comparison between FDI TMS mapping results of first and second session. Individual results of two consecutive FDI TMS mapping sessions (1 and 2) of all subjects. Colors indicate the resulting RMTs at the respective targets (% MSO). CoGs are marked with red dots.

entirely randomized. Time dependent changes would have therefore affected all targets. As we further used a similar experimental protocol AHH, MAM and MHS, changes of cortical alertness between the sessions might have influenced the inter-session CoG shift but should not have biased the comparison between procedures.

Another factor that influences TMS measurements is the rotation angle of the TMS coil. Each target and muscle representation has a specific optimal coil rotation angle, which depends on individual neuroanatomy (Bashir et al., 2013; Guggisberg et al., 2001). In the present study the robot maintained a constant rotation angle at each target and during the entire experiment in order to assure comparability between all targets. The rotation angle was set to 45°, which has been proven successful to date and is commonly used for TMS experiments (Mills et al., 1992; Ngomo et al., 2012; Pascual-Leone et al., 1994; Raffin et al., 2015). A more recently applied method to optimize coil positioning is to adjust the rotation of the TMS coil on the basis of individual neuroanatomy (Julkunen et al., 2009; Raffin et al., 2015; Weiss et al., 2012). However, a recent study found no advantage of either method (Raffin et al., 2015).

Nonetheless, the rotation of the TMS coil also influences the motor threshold (Raffin et al., 2015). Therefore, AHH would probably lead to the identification of targets with even lower thresholds with different coil rotation angles. To investigate this, the rotation angle could be theoretically introduced into the algorithm as an additional variable. Such a strategy would enable a systematic and unbiased assessment of the hotspot with the lowest threshold at an optimized rotation angle. However, as an additional variable would increase of the duration of the experiment considerably, we chose a defined rotation angle of 45° for the current study. The robot-aided identification of individually optimized rotation angles will be the aim of future studies.

If AHH needs to be improved with regards to duration of hotspot location, considerable time can be saved by reducing the number of pulses per grid point, shortening the inter-stimulus interval and/or decreasing the maximum stimulation intensity. With regard to the number of pulses per grid point our results indicate that accuracy in the range of a few millimeter is already achieved with a lower number of pulses per target. E.g. 3 pulses per target led to an average accuracy of 1.8 mm (SEM: 0.2) and a mean inter-session CoG shift of 2.4 mm (SEM: 0.3) within approx. 15 min.

In conclusion, AHH is able to improve TMS measurements whenever neuroanatomical precision and reliability are required, such as the exact identification of the location of the motor hotspots of different muscles

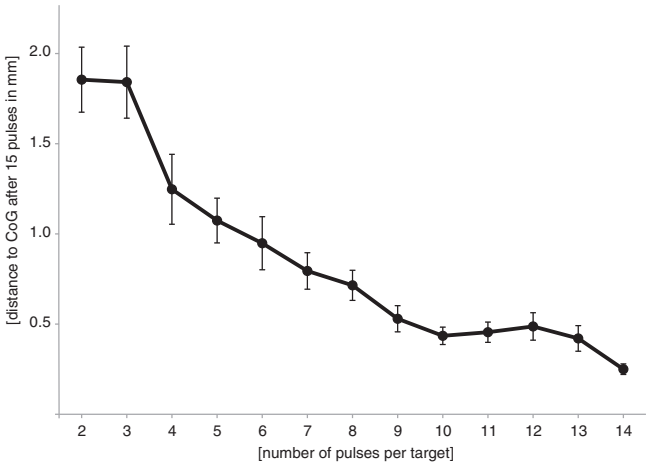

Fig. 6. Accuracy of AHH depends on the number of stimuli used for threshold estimation. CoGs were calculated from threshold estimates after x pulses per target (x-axis). The distance between these calculated CoGs and the final CoG (after 15 pulses) negatively correlates with the number of stimuli per target. After 9 pulses per target increasing the number of pulses did not further improve the accuracy of CoG location (floor effect). Error bars indicate SEM.

as well as excitability studies where the hotspot of a target muscle is located repeatedly. The co-registration of the subjects' head with individual MRI data further allows that a once identified hotspot can be re-located within few minutes without repeating the hotspot search. By introducing additional variables into the algorithm, such as different rotation angles, AHH provides new opportunities for the optimization of TMS coil positioning.

Acknowledgments

This study was partly funded by the German Federal Ministry of Education and Research (FKZ 01EZ1122A) and the German Federal Ministry for Economic Affairs and Energy (KF 2046402FO9). We thank C. Crozier for improving the English.

References

Awiszus, F., 2003. TMS and threshold hunting. Suppl. Clin. Neurophysiol. 56, 13–23.
Awiszus, F., 2011. Fast estimation of transcranial magnetic stimulation motor threshold: is it safe? Brain Stimul. 4, 58–59 (discussion 60–53).
Barker, A.T., Jalinous, R., Freeston, I.L., 1985. Non-invasive magnetic stimulation of human motor cortex. Lancet 1, 1106–1107.
Bashir, S., Perez, J.M., Horvath, J.C., Pascual-Leone, A., 2013. Differentiation of motor cortical representation of hand muscles by navigated mapping of optimal TMS current directions in healthy subjects. J. Clin. Neurophysiol. 30, 390–395.
Brasil-Neto, J.P., McShane, L.M., Fuhr, P., Hallett, M., Cohen, L.G., 1992. Topographic mapping of the human motor cortex with magnetic stimulation: factors affecting accuracy and reproducibility. Electroencephalogr. Clin. Neurophysiol. 85, 9–16.
Cincotta, M., Giovannelli, F., Borgheresi, A., Balestrieri, F., Toscani, L., Zaccara, G., Carducci, F., Viggiano, M.P., Rossi, S., 2010. Optically tracked neuronavigation increases the stability of hand-held focal coil positioning: evidence from "transcranial" magnetic stimulation-induced electrical field measurements. Brain Stimul. 3, 119–123.
Conforto, A.B., Z'Graggen, W.J., Kohl, A.S., Rosler, K.M., Kaelin-Lang, A., 2004. Impact of coil position and electrophysiological monitoring on determination of motor thresholds to transcranial magnetic stimulation. Clin. Neurophysiol. 115, 812–819.
Di Lazzaro, V., Ziemann, U., 2013. The contribution of transcranial magnetic stimulation in the functional evaluation of microcircuits in human motor cortex. Front. Neural. Circuits 7, 18.
Di Lazzaro, V., Oliviero, A., Profice, P., Saturno, E., Pilato, F., Insola, A., Mazzone, P., Tonali, P., Rothwell, J.C., 1998a. Comparison of descending volleys evoked by transcranial magnetic and electric stimulation in conscious humans. Electroencephalogr. Clin. Neurophysiol. 109, 397–401.
Di Lazzaro, V., Restuccia, D., Oliviero, A., Profice, P., Ferrara, L., Insola, A., Mazzone, P., Tonali, P., Rothwell, J.C., 1998b. Effects of voluntary contraction on descending volleys evoked by transcranial stimulation in conscious humans. J. Physiol. 508 (Pt 2), 625–633.
Di Lazzaro, V., Oliviero, A., Saturno, E., Pilato, F., Insola, A., Mazzone, P., Profice, P., Tonali, P., Rothwell, J.C., 2001. The effect on corticospinal volleys of reversing the direction of current induced in the motor cortex by transcranial magnetic stimulation. Exp. Brain Res. 138, 268–273.
Doeltgen, S.H., Ridding, M.C., 2010. Behavioural exposure and sleep do not modify corticospinal and intracortical excitability in the human motor system. Clin. Neurophysiol. 121, 448–452.
Ellaway, P.H., Davey, N.J., Maskill, D.W., Rawlinson, S.R., Lewis, H.S., Anissimova, N.P., 1998. Variability in the amplitude of skeletal muscle responses to magnetic stimulation of the motor cortex in man. Electroencephalogr. Clin. Neurophysiol. 109, 104–113.
Grundey, J., Thirugnanasambandam, N., Kaminsky, K., Drees, A., Skwirba, A.C., Lang, N., Paulus, W., Nitsche, M.A., 2012. Neuroplasticity in cigarette smokers is altered under withdrawal and partially restituted by nicotine exposition. J. Neurosci. 32, 4156–4162.
Guerra, A., Petrichella, S., Vollero, L., Ponzo, D., Pasqualetti, P., Maatta, S., Mervaala, E., Kononen, M., Bressi, F., Iannello, G., Rossini, P.M., Ferreri, F., 2014. Neurophysiological features of motor cortex excitability and plasticity in Subcortical Ischemic Vascular Dementia: a TMS mapping study. Clin. Neurophysiol. 126, 906–913.
Guggisberg, A.G., Dubach, P., Hess, C.W., Wuthrich, C., Mathis, J., 2001. Motor evoked potentials from masseter muscle induced by transcranial magnetic stimulation of the pyramidal tract: the importance of coil orientation. Clin. Neurophysiol. 112, 2312–2319.
Gugino, L.D., Romero, J.R., Aglio, L., Titone, D., Ramirez, M., Pascual-Leone, A., Grimson, E., Weisenfeld, N., Kikinis, R., Shenton, M.E., 2001. Transcranial magnetic stimulation coregistered with MRI: a comparison of a guided versus blind stimulation technique and its effect on evoked compound muscle action potentials. Clin. Neurophysiol. 112, 1781–1792.
Julkunen, P., Saisanen, L., Danner, N., Niskanen, E., Hukkanen, T., Mervaala, E., Kononen, M., 2009. Comparison of navigated and non-navigated transcranial magnetic stimulation for motor cortex mapping, motor threshold and motor evoked potentials. NeuroImage 44, 790–795.
Jung, N.H., Delvendahl, I., Kuhnke, N.G., Hauschke, D., Stolle, S., Mall, V., 2010. Navigated transcranial magnetic stimulation does not decrease the variability of motor-evoked potentials. Brain Stimul. 3, 87–94.
Kantelhardt, S.R., Fadini, T., Finke, M., Kallenberg, K., Siemerkus, J., Bockermann, V., Matthaeus, L., Paulus, W., Schweikard, A., Rohde, V., Giese, A., 2010. Robot-assisted image-guided transcranial magnetic stimulation for somatotopic mapping of the motor cortex: a clinical pilot study. Acta Neurochir. (Wien) 152, 333–343.
Kiers, L., Cros, D., Chiappa, K.H., Fang, J., 1993. Variability of motor potentials evoked by transcranial magnetic stimulation. Electroencephalogr. Clin. Neurophysiol. 89, 415–423.
Lancaster, J.L., Narayana, S., Wenzel, D., Luckemeyer, J., Roby, J., Fox, P., 2004. Evaluation of an image-guided, robotically positioned transcranial magnetic stimulation system. Hum. Brain Mapp. 22, 329–340.
Lang, N., Rothkegel, H., Reiber, H., Hasan, A., Sueske, E., Tergau, F., Ehrenreich, H., Wuttke, W., Paulus, W., 2011. Circadian modulation of GABA-mediated cortical inhibition. Cereb. Cortex 21, 2299–2306.
Lang, N., Rothkegel, H., Peckolt, H., Deuschl, G., 2013. Effects of lacosamide and carbamazepine on human motor cortex excitability: a double-blind, placebo-controlled transcranial magnetic stimulation study. Seizure 22, 726–730.
Littmann, A.E., McHenry, C.L., Shields, R.K., 2013. Variability of motor cortical excitability using a novel mapping procedure. J. Neurosci. Methods 214, 137–143.
Lotze, M., Kaethner, R.J., Erb, M., Cohen, L.G., Grodd, W., Topka, H., 2003. Comparison of representational maps using functional magnetic resonance imaging and transcranial magnetic stimulation. Clin. Neurophysiol. 114, 306–312.
Malcolm, M.P., Triggs, W.J., Light, K.E., Shechtman, O., Khandekar, G., Gonzalez Rothi, L.J., 2006. Reliability of motor cortex transcranial magnetic stimulation in four muscle representations. Clin. Neurophysiol. 117, 1037–1046.
Mills, K.R., Boniface, S.J., Schubert, M., 1992. Magnetic brain stimulation with a double coil: the importance of coil orientation. Electroencephalogr. Clin. Neurophysiol. 85, 17–21.
Ngomo, S., Leonard, G., Moffet, H., Mercier, C., 2012. Comparison of transcranial magnetic stimulation measures obtained at rest and under active conditions and their reliability. J. Neurosci. Methods 205, 65–71.
Oldfield, R.C., 1971. The assessment and analysis of handedness: the Edinburgh inventory. Neuropsychologia 9, 97–113.
Pascual-Leone, A., Cohen, L.G., Brasil-Neto, J.P., Hallett, M., 1994. Non-invasive differentiation of motor cortical representation of hand muscles by mapping of optimal current directions. Electroencephalogr. Clin. Neurophysiol. 93, 42–48.
Raffin, E., Pellegrino, G., Di Lazzaro, V., Thielscher, A., Siebner, H.R., 2015. Bringing transcranial mapping into shape: sulcus-aligned mapping captures motor somatotopy in human primary motor hand area. NeuroImage 120, 164–175.
Richter, L., Neumann, G., Oung, S., Schweikard, A., Trillenberg, P., 2013a. Optimal coil orientation for transcranial magnetic stimulation. PLoS One 8, e60358.
Richter, L., Trillenberg, P., Schweikard, A., Schlaefer, A., 2013b. Stimulus intensity for hand held and robotic transcranial magnetic stimulation. Brain Stimul. 6, 315–321.
Rossini, P.M., Barker, A.T., Berardelli, A., Caramia, M.D., Caruso, G., Cracco, R.Q., Dimitrijevic, M.R., Hallett, M., Katayama, Y., Lucking, C.H., et al., 1994. Non-invasive electrical and magnetic stimulation of the brain, spinal cord and roots: basic principles and procedures for routine clinical application. Report of an IFCN committee. Electroencephalogr. Clin. Neurophysiol. 91, 79–92.
Schmidt, S., Bathe-Peters, R., Fleischmann, R., Ronnefarth, M., Scholz, M., Brandt, S.A., 2015. Nonphysiological factors in navigated TMS studies; confounding covariates and valid intracortical estimates. Hum. Brain Mapp. 36, 40–49.
Siebner, H.R., Ziemann, U., 2014. What is the threshold for developing and applying optimized procedures to determine the corticomotor threshold? Clin. Neurophysiol. 125, 1–2.
Sparing, R., Buelte, D., Meister, I.G., Paus, T., Fink, G.R., 2008. Transcranial magnetic stimulation and the challenge of coil placement: a comparison of conventional and stereotaxic neuronavigational strategies. Hum. Brain Mapp. 29, 82–96.

Tamm, A.S., Lagerquist, O., Ley, A.L., Collins, D.F., 2009. Chronotype influences diurnal variations in the excitability of the human motor cortex and the ability to generate torque during a maximum voluntary contraction. J. Biol. Rhythms 24, 211–224.
Thielscher, A., Opitz, A., Windhoff, M., 2011. Impact of the gyral geometry on the electric field induced by transcranial magnetic stimulation. NeuroImage 54, 234–243.
van de Ruit, M., Perenboom, M.J., Grey, M.J., 2014. TMS brain mapping in less than two minutes. Brain Stimul. 8, 231–239.
Volz, L.J., Hamada, M., Rothwell, J.C., Grefkes, C., 2014. What makes the muscle twitch: motor system connectivity and TMS-induced activity. Cereb. Cortex 25, 2346–2353.
Wassermann, E.M., 2002. Variation in the response to transcranial magnetic brain stimulation in the general population. Clin. Neurophysiol. 113, 1165–1171.
Wassermann, E.M., McShane, L.M., Hallett, M., Cohen, L.G., 1992. Noninvasive mapping of muscle representations in human motor cortex. Electroencephalogr. Clin. Neurophysiol. 85, 1–8.
Wassermann, E.M., Pascual-Leone, A., Hallett, M., 1994. Cortical motor representation of the ipsilateral hand and arm. Exp. Brain Res. 100, 121–132.
Weiss, C., Nettekoven, C., Rehme, A.K., Neuschmelting, V., Eisenbeis, A., Goldbrunner, R., Grefkes, C., 2012. Mapping the hand, foot and face representations in the primary motor cortex—retest reliability of neuronavigated TMS versus functional MRI. NeuroImage 66C, 531–542.
Weiss, C., Nettekoven, C., Rehme, A.K., Neuschmelting, V., Eisenbeis, A., Goldbrunner, R., Grefkes, C., 2013. Mapping the hand, foot and face representations in the primary motor cortex—retest reliability of neuronavigated TMS versus functional MRI. NeuroImage 66, 531–542.
Wolf, S.L., Butler, A.J., Campana, G.I., Parris, T.A., Struys, D.M., Weinstein, S.R., Weiss, P., 2004. Intra-subject reliability of parameters contributing to maps generated by transcranial magnetic stimulation in able-bodied adults. Clin. Neurophysiol. 115, 1740–1747.